Supporting Information

Tuning N-donor Coordination and Assembly Structures in Uranyl Compounds of Carboxylate Ligands with Divergent Vinyl Pyridine Groups

Meng-ran Song,[a] Qun-yan Wu,*[b] Wei Jin,[b] Zhi-wei Huang,[b] Kong-qiu Hu,[b] Li-yong Yuan,[b] Wei Wen,*[a] Wei-qun Shi,[b c] and Lei Mei*[b]

[a] *Laboratory for the Synthesis and Application of Organic Functional Molecules & College of Chemistry and Chemical Engineering, Hubei University, Wuhan, 430062, PR China.*

[b] *Laboratory of Nuclear Energy Chemistry, Institute of High Energy Physics, Chinese Academy of Sciences, Beijing 100049, PR China.*

[c] *School of Nuclear Science and Engineering, Shanghai Jiao Tong University, Shanghai 200240, PR China.*

Table of Contents

S1. Supplementary Methods

S2. Supplementary Figures

Figure S1. The asymmetric units of **1-6**.

Figure S2. The surrounding coordination sphere of each uranyl center in **1** containing two bridging hydroxyl groups, two O atoms from different bridging carboxyl groups of two [pPyVB]$^-$ linkers, and a N-donor from another [pPyVB]$^-$ linker: (A) stick model; (B) polyhedral model.

Figure S3. Hydrogen bonds between two adjacent 2D layers in **1** (O3-H6, 2.636(6) Å; O2-H14, 2.838(5) Å).

Figure S4. Lattice stacking and hydrogen interactions of two uranyl moieties in **2**: (A-C) the supramolecular 3D framework formed by alternating supramolecular networks of tetra-nuclear chains and mono-nuclear complex (A) with two different arrays, tetranuclear uranyl moieties (B) and mononuclear uranyl moieties (C); (D) hydrogen bonds between adjacent uranyl moieties (O4···H33 distance, 2.673(4) Å; O3···H28 distance, 2.426(5) Å; O3···H27 distance, 2.946(4) Å; O1···H27 distance, 2.826(7) Å; O1···H29 distance, 2.306(5) Å; O1···H36 distance, 2.611(4) Å).

Figure S5. Hydrogen bonds between adjacent uranyl-based four-member rectangular units for constructing final supramolecular chains and networks.

Figure S6. The possible formation mechanism of terephthalate from MPyVB through the oxidative cleavage of olefins into carboxylic acids by ambient oxygen under hydrothermal/solvent conditions.

Figure S7. (A) C-H···O hydrogen bonds between adjacent basic structural units in **4** (O2···H6 distance, 2.595(4) Å; O2···H9 distance, 2.703(3) Å); (B) C-H···O hydrogen bonds between adjacent basic structural units in **5** (O2···H6 distance, 3.003(6) Å; O2···H9 distance, 3.044(7) Å).

Figure S8. Lattice packing of **4** (A-C) and **5** (D-F).

Figure S9. Molecular structure of **3** with the labels of U, O and N atoms for bonding analysis.

Figure S10. The simulated and experimental PXRD patterns of **1**.

Figure S11. The simulated and experimental PXRD patterns of **2**.

Figure S12. The simulated and experimental PXRD patterns of **3**.

Figure S13. The simulated and experimental PXRD patterns of **4**.

Figure S14. The simulated and experimental PXRD patterns of **5**.

Figure S15. The simulated and experimental PXRD patterns of **6**.

Figure S16. Thermogravimetric results of **1-6**.

Figure S17. FT-IR spectra of **1-6**.

Figure S18. The set-up for the iodine absorption experiments.

S3. Supplementary Tables

Table S1. Synthetic information for UCPs 1-6

Table S2. Selected bond distances (Å) of U-O and U-N bonds in **1-6**.

Table S3. A comparison in N-involved uranyl coordination sphere and extended strucuture of uranyl compounds based on different pyridine carboxylic acid ligands including isonicotinic acid, 3,5-dichloroisonicotinic acid, (E)-3-(Pyridin-4-yl)acrylic acid, HpPyVB and HmyVB.

Table S4. The values of WBI, GJBO and NMBO for the U-O/N bonds at BP86/ZORA/TZ2P level of theory.

Table S5. Kinetic parameters for gaseous iodine adsorption on **1** and **2**.

S4. Supplementary References

S1. Supplementary Methods

Materials and Methods

Caution! Because of the radioactive and chemically toxic nature of uranyl nitrate hexahydrate, $UO_2(NO_3)_2\cdot6H_2O$, precautions with suitable care and protection should be followed. All chemical reagents are purchased commercially and used directly without further purification. $UO_2(NO_3)_2\cdot6H_2O$ (12.55 g, 0.025 mol) was dissolved in 50 mL of deionized water to afford 0.5 M uranyl nitrate mother liquor. The experimental data of powder X-ray diffraction (PXRD) were collected on the Bruker D8 Advance powder X-ray diffractometer. The copper target provided Kα rays (λ = 1.5406 Å) with a step length of 0.02°. Thermogravimetric analysis (TGA) uses a model TA Q500 analyzer; the recorded temperature range is 30-800 °C, and the heating rate is 5 °C/min. The infrared (IR) data were recorded with the Bruker Tensor 27 infrared spectrometer, and the measurement range is 400-4000 cm^{-1}. Fluorescence spectra were recorded on a Hitachi F-4600 fluorescence spectrophotometer. Ultraviolet-visible (UV-vis) absorption spectroscopy was performed with a HITACHI U-3600 instrument.

Synthesis of Ligands

HpPyVB: The ligand was synthesized according to the previously reported literature with a minor modification[1]. 4-formylbenzoic acid (8.0 g, 0.053 mmol) and 4-methylpyridine (5.22 mL, 0.054 mmol) were refluxed in 25 mL acetic anhydride for 16 hours. The mixture was then cooled to ambient temperature and poured onto 200 mL of ice water. A light-yellow powder was collected from filtration, and washed repeatedly with water, followed by aqueous ethanol, and dried to give (E)-4-(2-(pyridin-4-yl)vinyl)benzoic acid (HpPyVB) (11.5 g, 96.3%).1H NMR (500 MHz, 25°C, DMSO-d6): δ/ppm = 12.95 (br, 1H), 8.52 (d, 2H), 7.97 (d, 2H), 7.77 (d, 2H), 7.66 (d, 1H), 7.63 (d, 2H), 7.41 (d, 1H).IR data (KBr, cm^{-1}): 3008, 1637, 1674, 1414, 1161, 1127, 1034, 1012, 942, 843, 812, 764, 743, 634, 512.

HmPyVB: The ligand was synthesized according to the previously reported literature with a minor modification[1]. 3-formylbenzoic acid (8.0 g, 0.053 mmol) and 4-

methylpyridine (5.22 mL, 0.054 mmol) were refluxed in 25 mL acetic anhydride for 16 hours. The mixture was then cooled to ambient temperature and poured onto 200 mL of ice water. A brownish-yellow powder was collected from filtration, and washed repeatedly with water, followed by aqueous ethanol, and dried to give (E)-3-(2-(pyridin-4-yl)vinyl)benzoic acid (HmPyVB) (10.85g, 90.9%).1H NMR (500 MHz, 25℃, DMSO-d6): δ/ppm =13.16 (s, 1H), 8.54 (d, 2H), 8.25 (s, 1H), 7.92 (t, 2H), 7.65 (d, 1H), 7.61 (d, 2H), 7.55 (t, 1H), 7.36 (d, 1H). IR data (KBr, cm^{-1}): 3028, 1686, 1606, 1414,1282, 1169, 1062, 1010, 952, 845, 811, 779, 763, 692, 592, 538, 518.

[HMPyVB]I: The ligand was synthesized according to the previously reported literature with a minor modification[2]. 1,4-dimethylpyridin-1-ium (12.69 g, 0.054 mol) iodide and 4-formylbenzoic acid (8.00 g, 0.053 mol) were refluxed in 25 mL acetic anhydride for 16 hours. The mixture was then cooled to ambient temperature and poured onto 200 mL of ice water. A light-yellow powder was collected from filtration, and washed repeatedly with water, followed by aqueous ethanol, and dried to give (E)-4-[2-(methylpyridin-4-yl)vinyl]benzoic acid ([HMPyVB]I) (13.9 g, 71.9%). 1H NMR (500 MHz, DMSO-d6): δ/ppm =13.14 (br, 1H), 8.91 (d, 2H), 8.27 (d, 2H), 8.07 (d, 1H), 8.03 (d, 2H), 7.85 (d, 2H), 7.67 (d, 1H), 4.21(s, 3H). IR data (KBr, cm^{-1}): 3389, 3037, 1703, 1644, 1622, 1564, 1519, 1502, 1415, 1368, 1334, 1257, 1217, 1178, 1108, 1010, 978, 959, 887,861, 821, 778, 751, 684, 640, 533, 518.

Bonding analysis and comparison of N-donors and O-donors

To explore the bonding nature between uranyl ions with N-donors and O-donors, **3** with [mPyVB]$^-$ ligands in two kinds of uranyl coordination modes was used as the representative model (Figure S9), and frontier molecular orbitals (MOs) and bond orders including Wiberg bond index (WBI),[3] Gophinatan-Jug bond order (GJBO)[4] and Nalewajski-Mrozek bond orders (NMBO)[5, 6] were carried out using BP86 functional with the Amsterdam Modeling Suite 2022 (AMS 2022)[7-9] Scalar-relativistic effects with the zeroth-order regular approximation (ZORA) Hamiltonian method and the Slater-type orbital (STO) all-electron TZ2P basis set[10] were applied.

Iodine Capture Experiment

To evaluate the sorption capacity of **1** and **2** for gaseous iodine, 20 mg of each was exposed to a saturated iodine vapor atmosphere at 75°C. Detailed experimental procedures are as followed (the set-up for the iodine absorption experiments is shown in Figure S18): a glass dish with 20 mg of **1** was placed in a sealed glass bottle containing 5 g of iodine and heated in an oven at 75 °C. The sample was periodically weighed until its mass stabilized. **2** was subjected to the same procedure as described above.

Experimental Data Fitting

The kinetic equations for the pseudo-primary and pseudo-secondary adsorption kinetic models are as follows.

Pseudo-first-order kinetic equations:

$$Q_t = Q_e - Q_e^{-K_1 \cdot t}$$

Pseudo-second-order kinetic equations:

$$Q_t = \frac{a^2 \cdot K_2 \cdot t}{1 + a \cdot K_2 \cdot t}$$

Here, K_1 (h^{-1}) and K_2 ($g \cdot mg^{-1} \cdot h^{-1}$) represent the first-order and second-order rate constants, respectively. Q_t ($mg \cdot g^{-1}$) denotes the iodine vapor adsorbed per gram of sample at time t, while Q_e ($mg \cdot g^{-1}$) represents the equilibrium adsorption capacity.

S2. Supplementary Figures

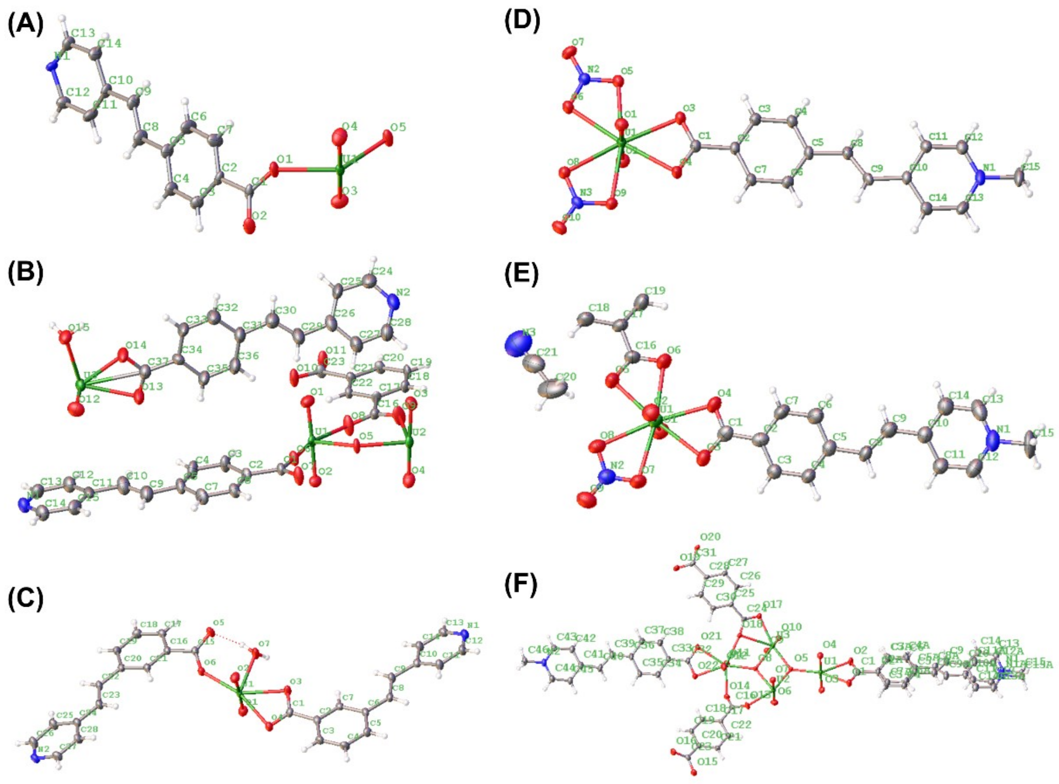

Figure S1. The asymmetric units of **1-6**.

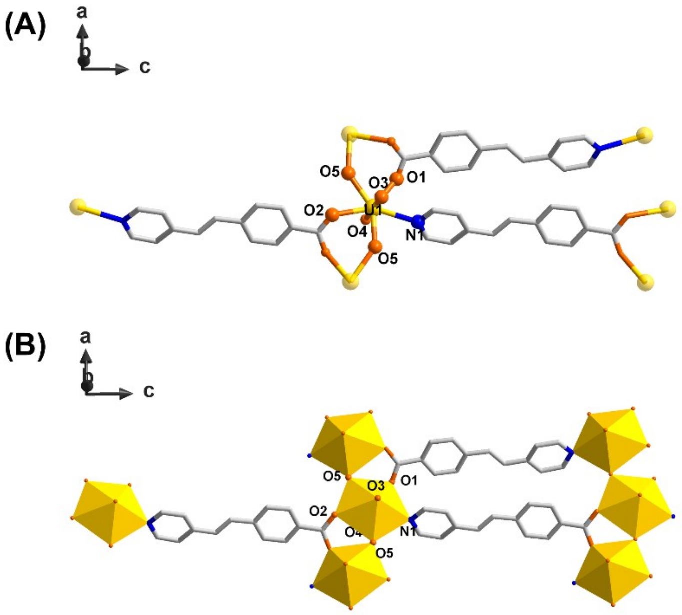

Figure S2. The surrounding coordination sphere of each uranyl center in **1** containing two bridging hydroxyl groups, two O atoms from different bridging carboxyl groups of two [pPyVB]$^-$ linkers, and a N-donor from another [pPyVB]$^-$ linker: (A) stick model; (B) polyhedral model.

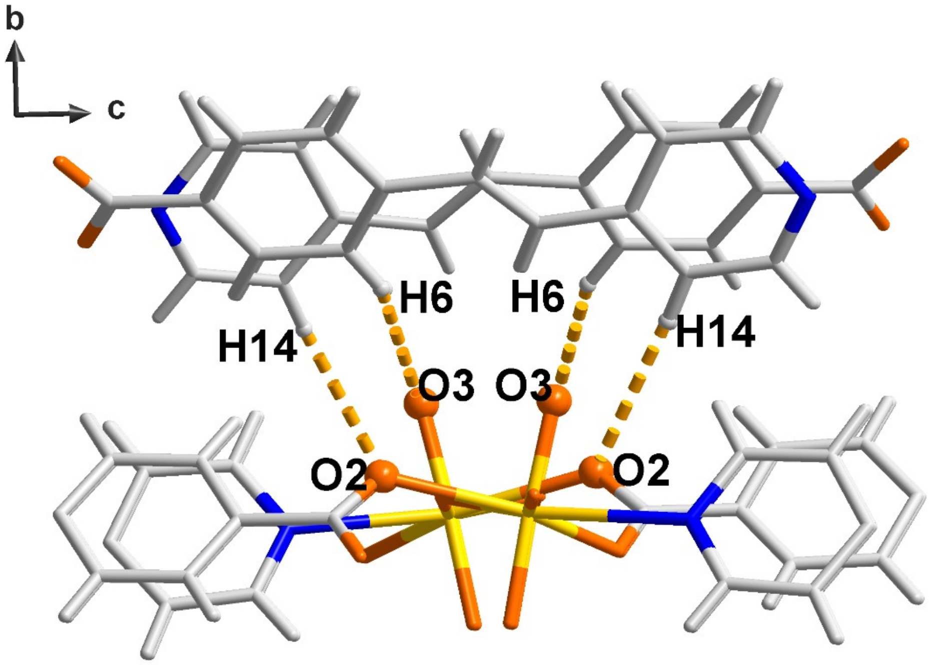

Figure S3. Hydrogen bonds between two adjacent 2D layers in **1** (O3-H6, 2.636(6) Å; O2-H14, 2.838(5) Å).

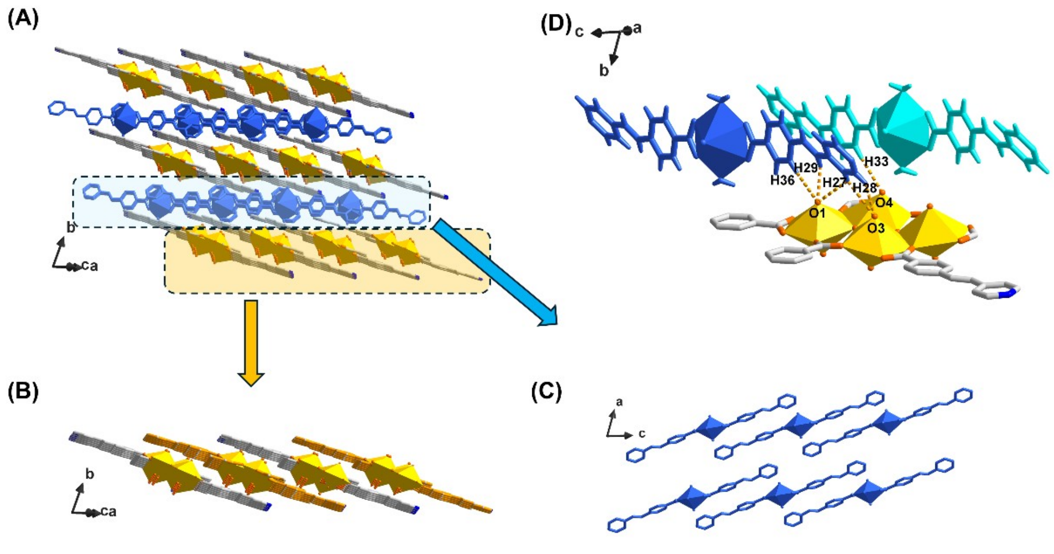

Figure S4. Lattice stacking and hydrogen interactions of two uranyl moieties in **2**: (A-C) the supramolecular 3D framework formed by alternating supramolecular networks of tetra-nuclear chains and mono-nuclear complex (A) with two different arrays, tetranuclear uranyl moieties (B) and mononuclear uranyl moieties (C); (D) hydrogen bonds between adjacent uranyl moieties (O4···H33 distance, 2.673(4) Å; O3···H28 distance, 2.426(5) Å; O3···H27 distance, 2.946(4) Å; O1···H27 distance, 2.826(7) Å; O1···H29 distance, 2.306(5) Å; O1···H36 distance, 2.611(4) Å).

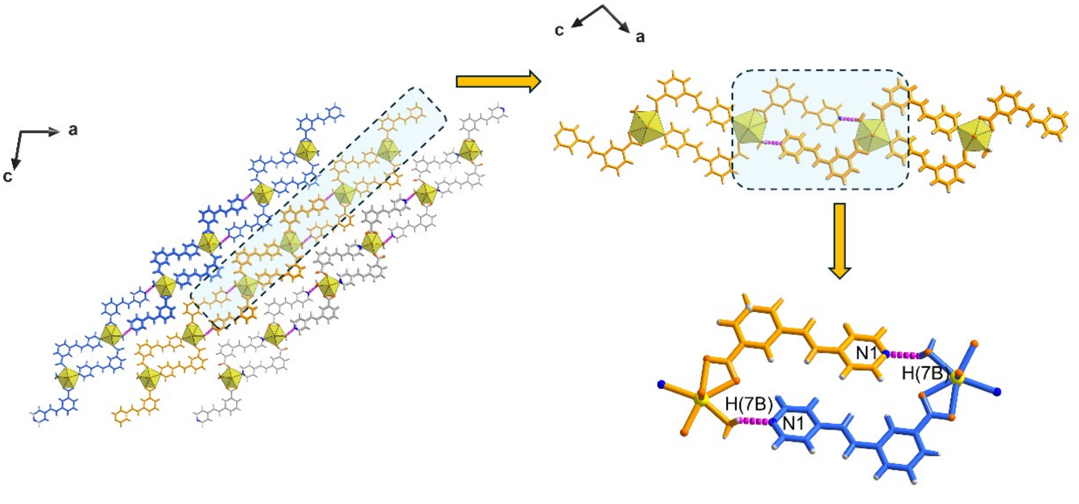

N1···H(7B): 2.312(4) Å

Figure S5. The O-H···N hydrogen bonds between adjacent uranyl-based four-member rectangular units for constructing final supramolecular chains and networks in **3**.

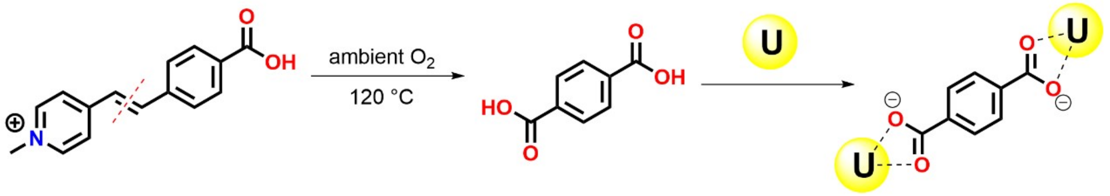

Figure S6. The possible formation mechanism of terephthalate from MPyVB through the oxidative cleavage of olefins into carboxylic acids by ambient oxygen under hydrothermal/solvent conditions.

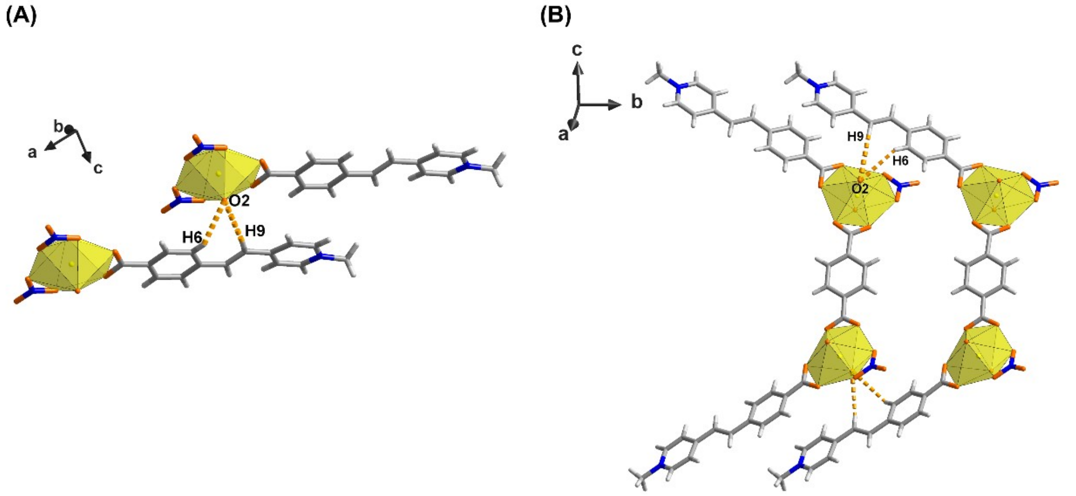

Figure S7. (A) C-H···O hydrogen bonds between adjacent basic structural units in **4** (O2···H6 distance, 2.595(4) Å; O2···H9 distance, 2.703(3) Å); (B) C-H···O hydrogen bonds between adjacent basic structural units in **5** (O2···H6 distance, 3.003(6) Å; O2···H9 distance, 3.044(7) Å).

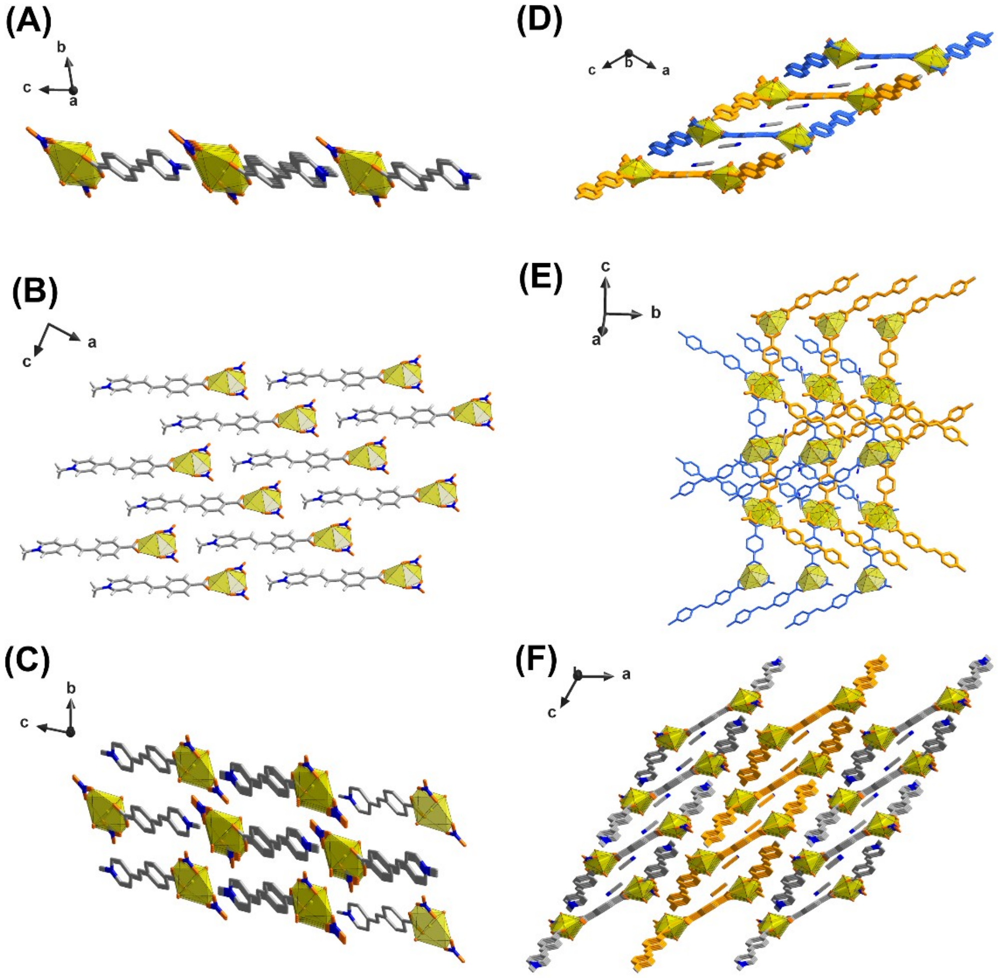

Figure S8. Lattice packing of **4** (A-C) and **5** (D-F).

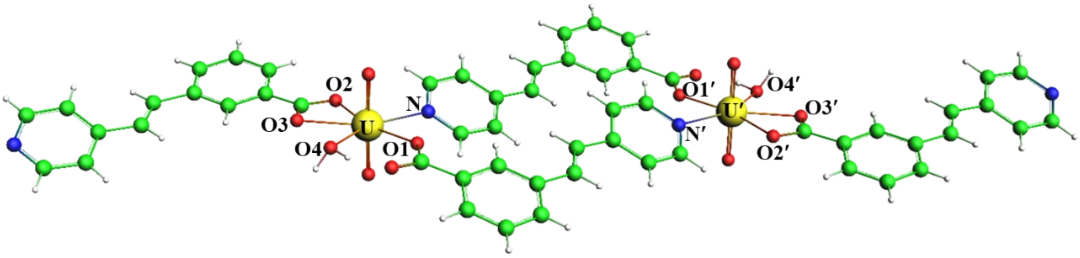

Figure S9. Molecular structure of **3** with the labels of U, O and N atoms for bonding analysis.

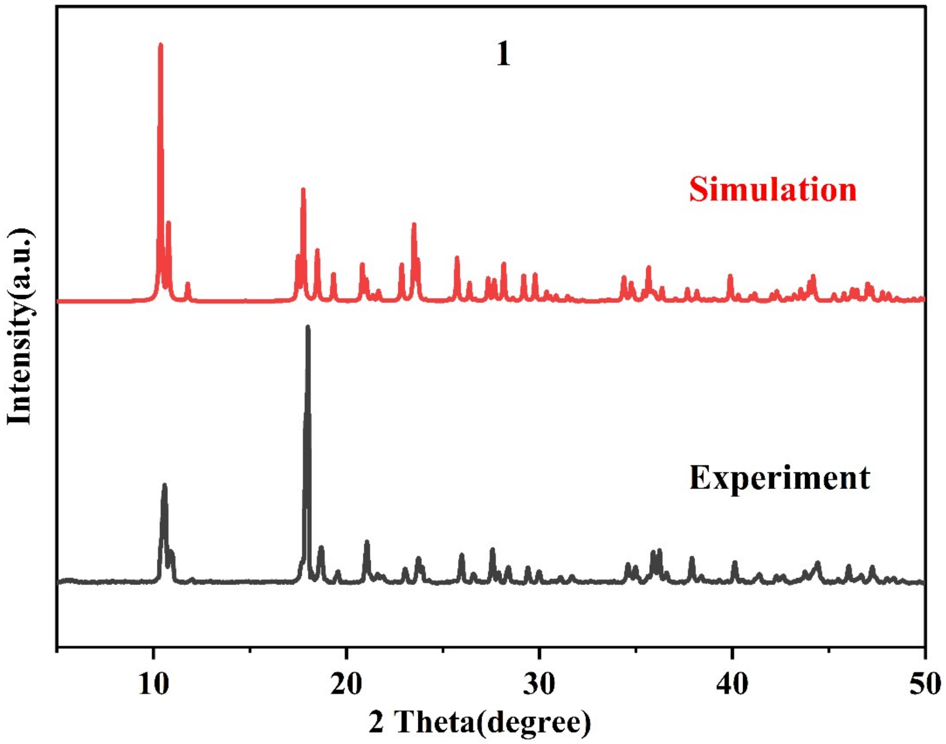

Figure S10. The simulated and experimental PXRD patterns of **1**.

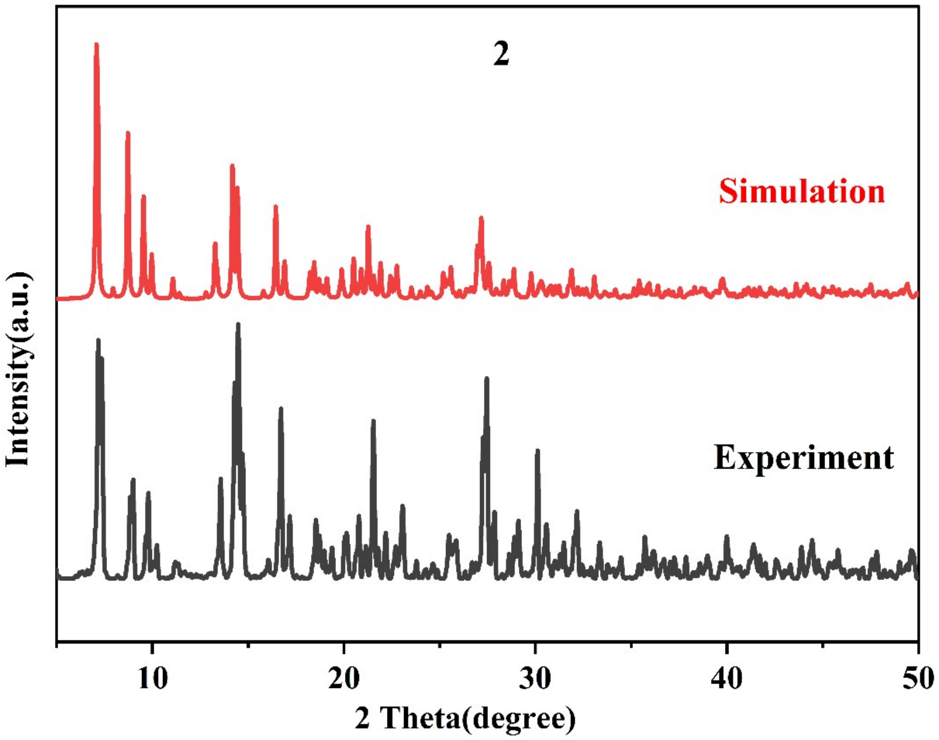

Figure S11. The simulated and experimental PXRD patterns of **2**.

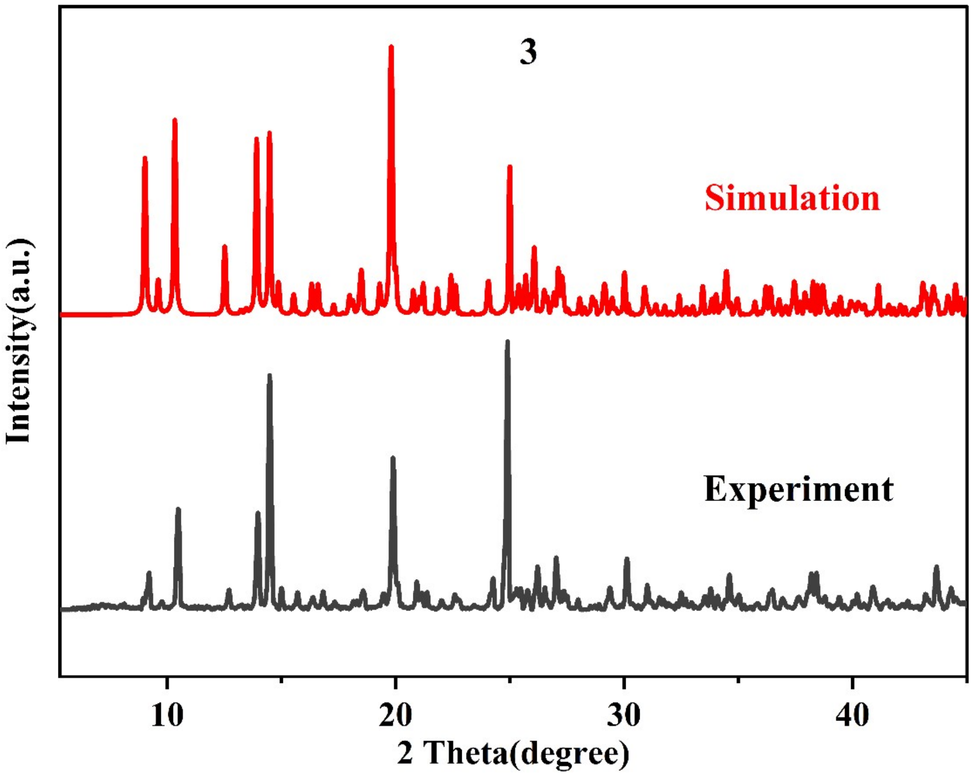

Figure S12. The simulated and experimental PXRD patterns of **3**.

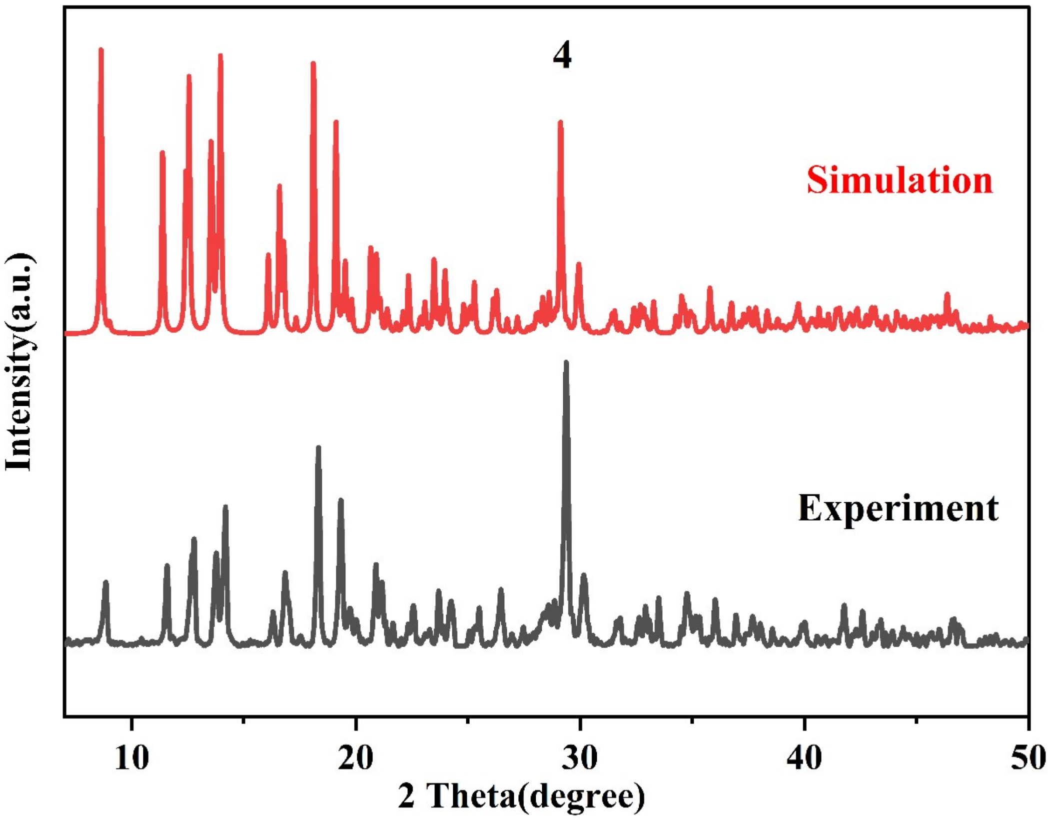

Figure S13. The simulated and experimental PXRD patterns of **4**.

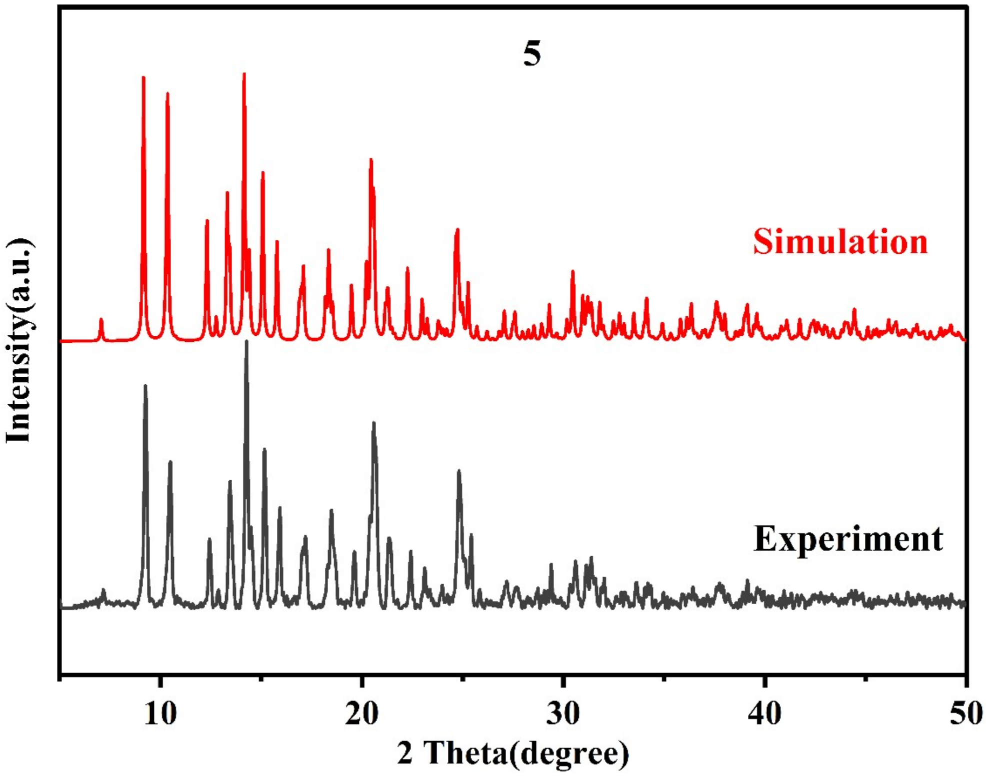

Figure S14. The simulated and experimental PXRD patterns of **5**.

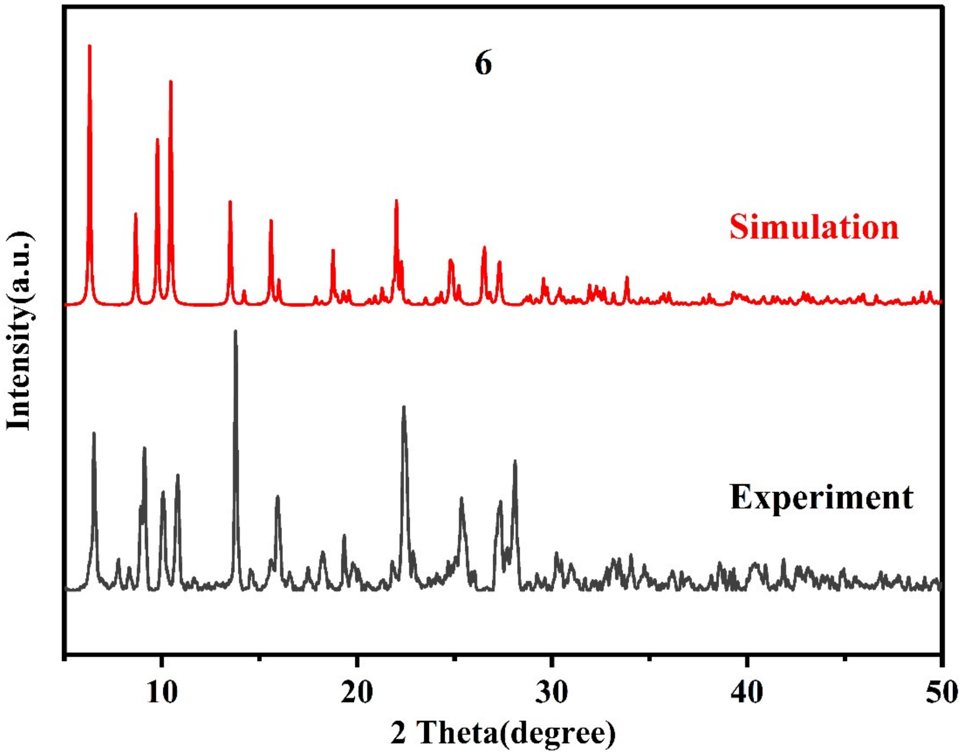

Figure S15. The simulated and experimental PXRD patterns of **6**.

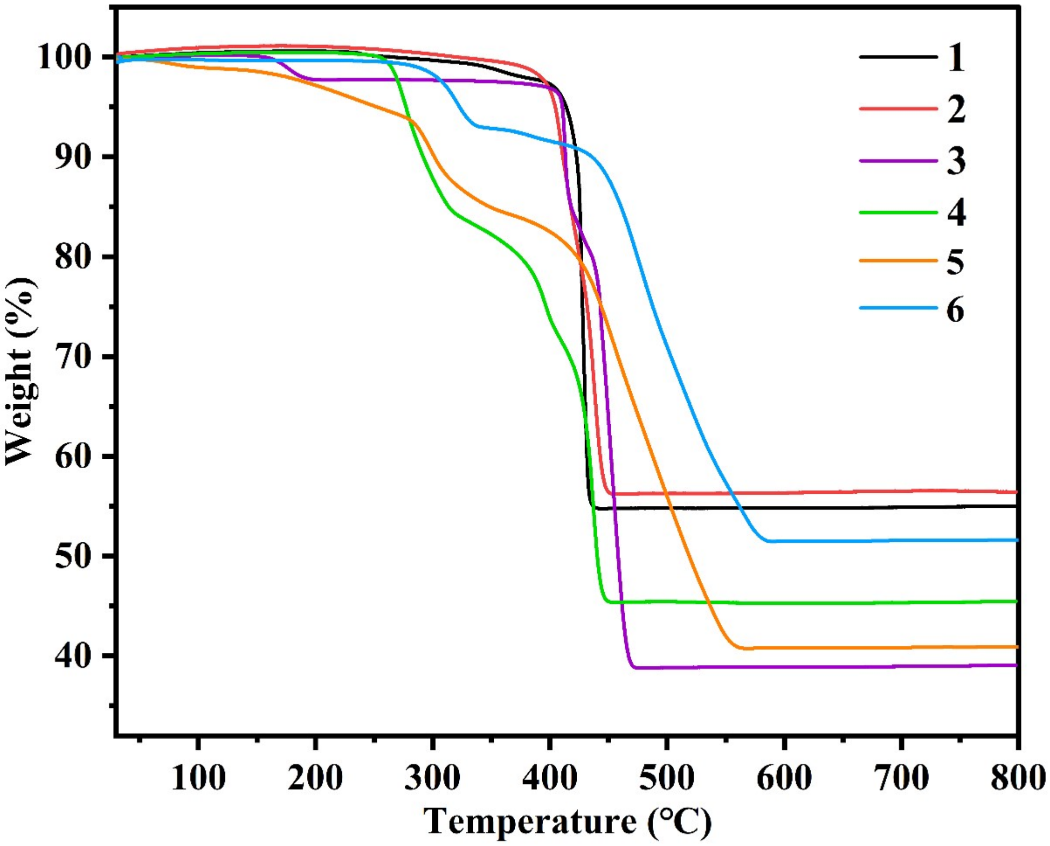

Figure S16. Thermogravimetric results of **1-6**.

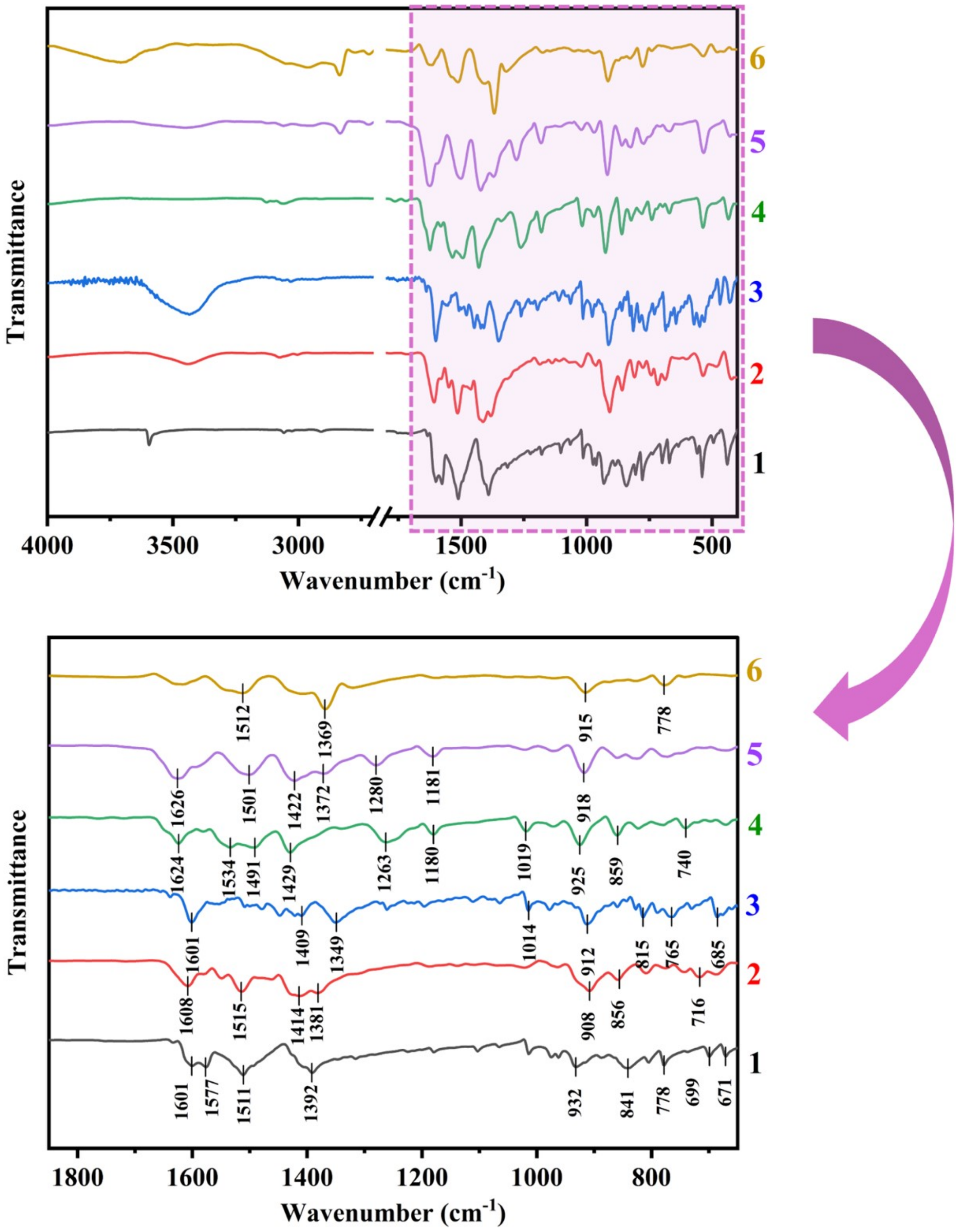

Figure S17. FT-IR spectra of **1-6**.

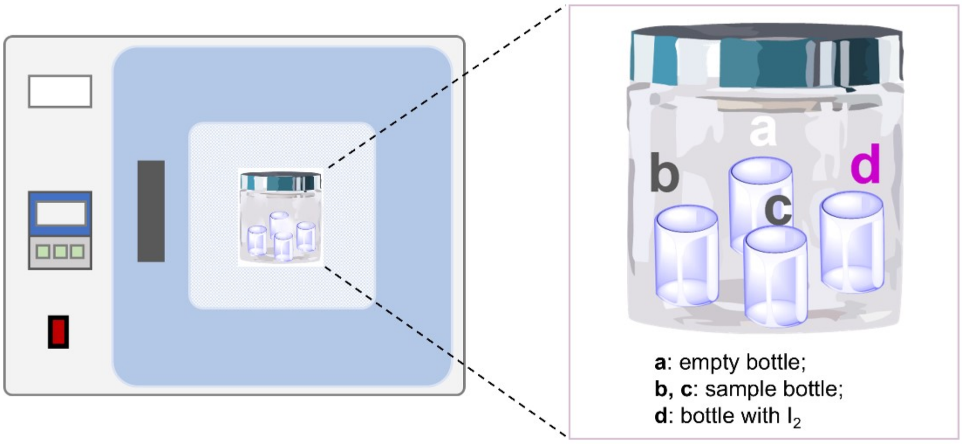

Figure S18. The set-up for the iodine absorption experiments.

S3. Supplementary Tables

Table S1. Synthetic information for complexes 1-6.

	1	**2**	**3**	**4**	**5**	**6**
$UO_2(NO_3)\cdot 6H_2O$ (mmol)	0.025	0.05	0.025	0.025	0.025	0.5
ligand (mmol)	0.025 (HpPyVB)	0.025 (HpPyVB), 0.025 （H_2ipht)	0.025 (HmPyVB)	0.025 ([HMPyVB]I)	0.05 ([HMPyVB]I)	0.025 ([HMPyVB]I), 0.025 (H_2tpht)
Solvent	CH_3CN/H_2O, 1.5 mL/0.5 mL	CH_3CN/H_2O, 1.5 mL/0.5 mL	DMF/H_2O, 2 mL/0.5 mL	CH_3CN, 2 mL	CH_3CN, 2 mL	H_2O, 2 mL
*p*H adj.	HNO_3(1 M) 20μL	None	HNO_3 (1 M) 280μL	None	HNO_3 (1 M) 100 μL	NaOH (1 M) 100 μL
Temp (°C)	150	150	150	120	120	150
Time (h)	48	48	24	72	72	48
color	Yellow	Yellow	Yellow	Yellow	Yellow	Yellow
Yield (%)	55.6	57.6	67.8	43.6	56.6	45.3

Table S2. Selected bond distances (Å) of U-O and U-N bonds in **1-6**.

1			
U1-O3	1.785(6)	U1-O4	1.763(6)
U1-O1	2.375(4)	U1-O4	2.427(4)
U1-O5	2.373(5)	U1-O5’	2.311(5)
U1-N1	2.621(5)		
2			
U1-O1	1.765(5)	U1-O2	1.783(5)
U1-O5	2.250(4)	U1-O6	2.443(5)
U1-O8	2.292(5)	U1-O10	2.457(5)
U1-O11	2.447(4)	U2-O3	1.775(5)
U2-O4	1.784(6)	U2-O5	2.255(4)
U2-O5’	2.254(4)	U2-O6	2.696(4)
U2-O7	2.465(5)	U2-O9	2.370(5)
U3-O12	1.755(6)	U3-O13	2.494(5)
U3-O14	2.415(5)	U3-O15	2.528(5)
3			
U1-O1	1.775(3)	U1-O2	1.770(3)
U1-O3	2.398(3)	U1-O4	2.485(3)
U1-O6	2.318(3)	U1-O7	2.341(3)
U1-N2	2.566(3)		
4			
U1-O1	1.766(3)	U1-O2	1.764(3)
U1-O8	2.488(3)	U1-O9	2.485(3)
U1-O5	2.478(3)	U1-O6	2.490(3)
U1-O3	2.424(3)	U1-O4	2.414(3)
5			
U1-O1	1.747(6)	U1-O2	1.747(6)
U1-O3	2.457(5)	U1-O4	2.415(5)

U1-O5	2.427(5)	U1-O6	2.467(6)
U1-O7	2.519(5)	U1-O8	2.542(6)
		6	
U1-O3	1.765(4)	U1-O4	1.763(4)
U1-O1	2.472(4)	U1-O2	2.478(4)
U1-O5	2.242(3)	U1-O15	2.355(3)
U1-O20	2.449(3)	U2-O5	2.252(3)
U2-O6	1.793(4)	U2-O7	1.784(4)
U2-O8	2.239(3)	U2-O13	2.334(3)
U2-O19	2.436(4)	U2-O20	2.698(3)
U3-O5	2.257(3)	U3-O8	2.253(3)
U3-O9	1.780(4)	U3-O10	1.781(4)
U3-O16	2.379(3)	U3-O17	2.469(3)
U3-O18	2.677(3)	U4-O8	2.241(3)
U4-O11	1.765(4)	U4-O12	1.778(4)
U4-O14	2.363(3)	U4-O18	2.482(3)
U4-O21	2.498(4)	U4-O22	2.455(4)

Table S3. A comparison in N-involved uranyl coordination sphere and extended structure of uranyl compounds based on different pyridine carboxylic acid ligands including isonicotinic acid, 3,5-dichloroisonicotinic acid, (E)-3-(Pyridin-4-yl)acrylic acid, HpPyVB and HmyVB.

Ligand	N-involved Uranyl Coordination Sphere	Extended Structure
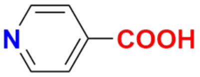 (RSC Advances, 2015, 5, 33249-33253)	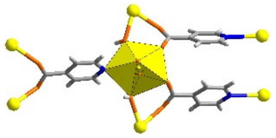	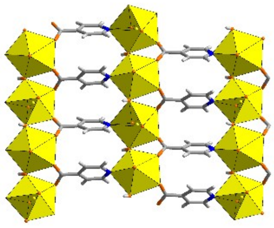
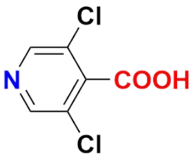 (*Cryst. Growth Des.*, 2015, **15**, 1395-1406)	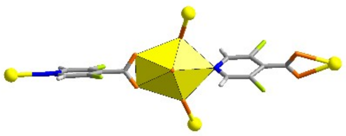	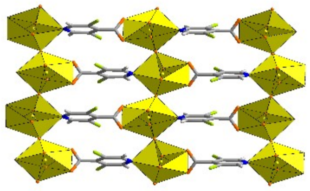
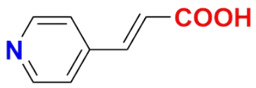 (*Inorg. Chem.*, 2018, **57**, 14772-14785)	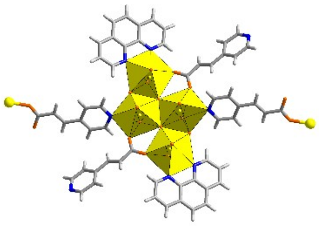	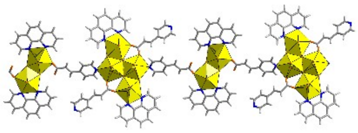
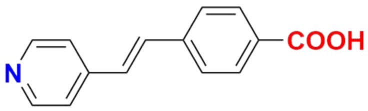 (this work)	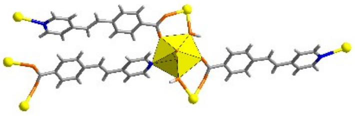	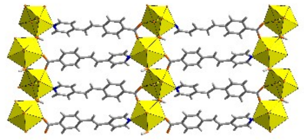
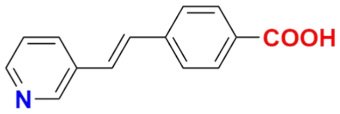 (this work)	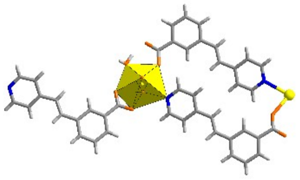	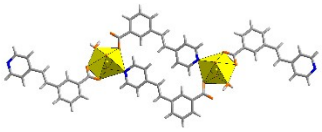

Table S4. The values of WBI, GJBO and NMBO for the U-O/N bonds at BP86/ZORA/TZ2P level of theory.

Bonds	**WBI**	**GJBO**	**NMBO**
U-N	0.371	0.422	0.491
U-O1	0.627	0.691	0.838
U-O2	0.437	0.462	0.568
U-O3	0.497	0.526	0.645
U-O4	0.444	0.467	0.603

Table S5. Kinetic parameters for gaseous iodine adsorption on **1** and **2**.

	Pseudo-first-order adsorption kinetics model			Pseudo-second-order adsorption kinetics model		
	Q_e ($mg \cdot g^{-1}$)	K_1 (h^{-1})	R^2	Q_e ($mg \cdot g^{-1}$)	K_2 ($g \cdot mg^{-1} \cdot h^{-1}$)	R^2
1	122	0.178	0.9908	131	0.0021	0.9951
2	100	0.743	0.9869	103	0.0144	0.9995

S4. Supplementary References

1. E. Elacqua, P. Kaushik, R. H. Groeneman, J. C. Sumrak, D.-K. Bučar and L. R. MacGillivray, *Angew. Chem. Int. Ed.*, 2012, **51**, 1037-1041.
2. J. S. Geng, L. Mei, Y. Y. Liang, L. Y. Yuan, J. P. Yu, K. Q. Hu, L. H. Yuan, W. Feng, Z. F. Chai and W. Q. Shi, *Nat. Commun.*, 2022, **13**, 2030.
3. K. B. Wiberg, *Tetrahedron*, 1968, **24**, 1083-1096.
4. M. S. Gopinathan and K. Jug, *Theor. Chim. Acta*, 1983, **63**, 497-509.
5. R. F. Nalewajski and J. Mrozek, *Int. J. Quantum Chem.*, 1994, **51**, 187-200.
6. R. F. Nalewajski, J. Mrozek and A. Michalak, *Int. J. Quantum Chem.*, 1997, **61**, 589-601.
7. C. Fonseca Guerra, J. Snijders, G. t. Te Velde and E. J. Baerends, *Thero. Chem. Acc.*, 1998, **99**, 391-403.
8. G. te Velde, F. M. Bickelhaupt, E. J. Baerends, C. Fonseca Guerra, S. J. A. van Gisbergen, J. G. Snijders and T. Ziegler, *J. Comput. Chem.*, 2001, **22**, 931-967.
9. T. Z. E.J. Baerends, J. Autschbach, D. Bashford, A. Bérces, F.M. Bickelhaupt, C. Bo, P.M. Boerrigter, L. Cavallo, D.P. Chong, L. Deng, R.M. Dickson, D.E. Ellis, M. van Faassen, L. Fan, T.H. Fischer, C. Fonseca Guerra, M. Franchini, A. Ghysels, A. Giammona, S.J.A. van Gisbergen, A.W. Götz, J.A. Groeneveld, O.V. Gritsenko, M. Grüning, S. Gusarov, F.E. Harris, P. van den Hoek, C.R. Jacob, H. Jacobsen, L. Jensen, J.W. Kaminski, G. van Kessel, F. Kootstra, A. Kovalenko, M.V. Krykunov, E. van Lenthe, D.A. McCormack, A. Michalak, M. Mitoraj, S.M. Morton, J. Neugebauer, V.P. Nicu, L. Noodleman, V.P. Osinga, S. Patchkovskii, M. Pavanello, P.H.T. Philipsen, D. Post, C.C. Pye, W. Ravenek, J.I. Rodríguez, P. Ros, P.R.T. Schipper, H. van Schoot, G. Schreckenbach, J.S. Seldenthuis, M. Seth, J.G. Snijders, M. Solà, M. Swart, D. Swerhone, G. te Velde, P. Vernooijs, L. Versluis, L. Visscher, O. Visser, F. Wang, T.A. Wesolowski, E.M. van Wezenbeek, G. Wiesenekker, S.K. Wolff, T.K. Woo, A.L. Yakovlev, ADF2022, SCM, Theoretical Chemistry, Vrije Universiteit, Amsterdam, The Netherlands.
10. E. Van Lenthe and E. J. Baerends, *J. Comput. Chem.*, 2003, **24**, 1142-1156.